Efficient Drug Delivering of a Photodynamic Therapy Agent into Cellular Membranes Rationalized by Molecular Dynamics

Basak Koca-Findik,[a,b] *Ilya Yakavets,*[c] *Henri-Pierre Lassalle,*[d,e] *Saron Catak,*[a] *Antonio Monari.*[b,*]

a) Bogazici University, Department of Chemistry, Bebek 34342, Istanbul, Turkey. b) Université Paris Cité and CNRS, ITODYS, F-75006, Paris, France. c) Department of Chemistry, University of Toronto, 80 Saint George Street, Toronto, Ontario M5S 3H6, Canada. d) Université de Lorraine and CNRS, CRAN, UMR 7039, F-54000, Nancy, France. e) Université de Lorraine, Institut de Cancérologie de Lorraine, F-54000, Nancy.

AUTHOR INFORMATION

Corresponding Author

*Antonio.monari@u-paris.fr

ABSTRACT. Photodynamic Therapy (PDT) represents a most attractive therapeutic strategy to reduce side effects of chemotherapy and improve the global quality of life of patients. Yet, many PDT drugs suffer from a poor bioavailability and cellular intake, and thus, drug delivery strategy should be implemented. In this letter we report the behavior of a temoporfin-based PDT drug, commercialized under the name of Foscan, complexed by two β-cyclodextrin units in presence of

a lipid bilayer. Our all atom simulations have shown the internalization of the complex and its spontaneous dissociation inside the lipid bilayer. The factors favoring penetration and dissociation have also been analyzed, together with the membrane perturbation due to the interaction with the cyclodextrin complex. Our results confirm the suitability of the encapsulation strategy for PDT, and rationalize the experimental results concerning its efficacy.

TOC GRAPHICS

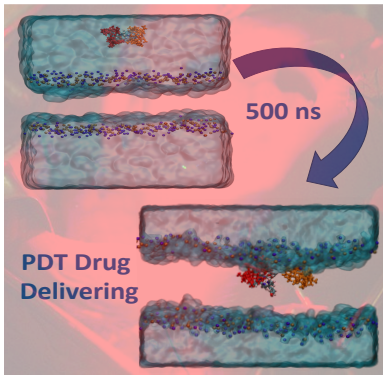

KEYWORDS Molecular Dynamics, Cyclodextrin encapsulation, Foscan, Lipid Membranes.

Photodynamic Therapy (PDT) is a promising therapeutic approach,[1–5] which combines the cytotoxic efficiency of a given drug with its activation by suitable electromagnetic radiation to improve the spatial and temporal selectivity of the treatment, and hence minimize side-effects. These features make PDT particularly promising in the field of cancer treatments,[2,6] allowing to bypass the usual systemic toxicity of conventional chemotherapeutic agents, such as cis-platin[7] and its derivatives,[8] which despite their efficiency induce important burdens on the quality of life of the patients. Furthermore, conventional chemotherapy agents may also lead to strong resistance

effects,[9,10] which result in a significant reduction of their efficiency and clinical applicability. From a fundamental point of view PDT relies in the administration of a drug which is inert in the dark, and thus of low toxicity. The excitation by suitable wavelengths induces the population of the drug excited states manifold which may afterwards produce reactive oxygen species (ROS). The latter will further attack biological macromolecular structures, such as lipid membranes, proteins, or nucleic acids, and, thus, lead to cell death.[11] One of the most common photophysical pathway exploited in PDT is the activation of molecular oxygen to its singlet excited state $^1O_2$, which has the capacity to easily oxidize biological molecules. The activation of molecular oxygen to $^1O_2$ requires the population of the drug's triplet states via intersystem crossing (ISC), whose facility and time-scale is therefore crucial in dictating its global efficiency. Other possible PDT strategies rely on the production of superoxide or peroxy-radicals, usually achieved through excited-state electron transfer paths.[12] Porphyrins and phthalocyanines are probably among the most common PDT agents exploited nowadays both in clinical applications and in research and development approaches.[5,13,14] This is mainly due to their high extinction coefficients and their facile ISC, which, furthermore, can be modulated by the suitable inclusion of heavy metal atoms, such as Pt, Zn, or Pd, in the coordination sphere constituted by the porphyrin core.[15,16]

Despite the clear success of PDT in cancer treatment, especially for esophageal, uterine and mouth cancers, as well as in the treatment of different viral,[17] bacterial,[18] and auto-immune diseases,[19] such as psoriasis,[20] PDT still suffers from some critical drawbacks, which should be properly considered.[21]

Indeed, the PDT drug should ideally absorb in the red and infrared portion of the electromagnetic spectrum, and specifically in the therapeutic window, i.e. the wavelengths to which biological tissues are transparent. This prerequisite is actually crucial to assure the highest penetration of the

activating light, and hence the treatment of deeper lesions. Furthermore, the accumulation of the drug into cancer cells is also needed to enhance the therapeutic efficiency of PDT. For this reasons, specific strategies based on the functionalization of PDT drugs with specific antibodies, targeting receptors which are over expressed on cancer cells, have been proposed.[22–24]

Nevertheless, an additional limitation occurs specifically for porphyrin-based PDT agents, which due to their extended hydrophobic π-conjugated system are prone to aggregation, thus strongly limiting their bioavailability and their possible oral or intravenous administration. Furthermore, aggregation may also significantly alter the photophysical properties of the drug, shifting the absorption spectrum maxima, and more importantly opening possible competitive pathways, impeding an efficient ISC, and thus $^1O_2$ activation.

As a matter of fact, a chlorin-based temoporfin (m-THCP, Figure 1),[25–27] commercialized under the name of Foscan, is one of the most efficient PDT agents, especially for the treatment of squamous cell head-and-neck cancer,[28,29] even in advanced stages and for palliative purposes.[30] Different studies, including pre-clinical and clinical tests, are also devoted to its possible use to treat other cancer types, including, for instance, ovarian cancer.[31] Despite its unquestionable success, m-THCP strongly suffers from aggregation issues, which severely limit its bioavailability.[32–35]

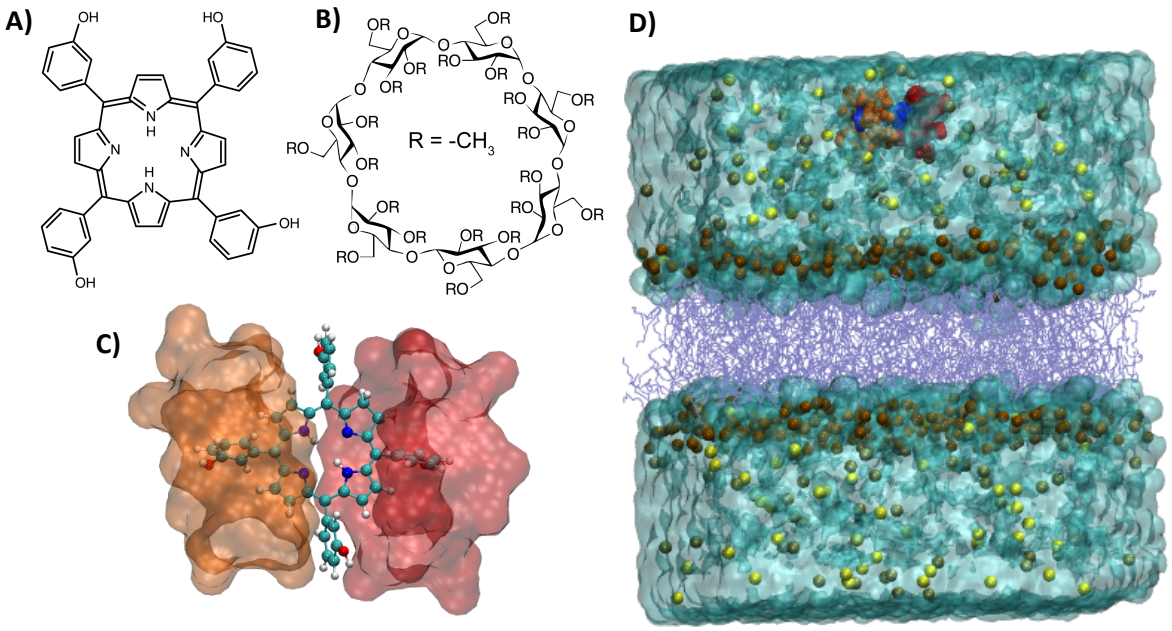

Figure 1. Chemical formula of m-THPC (A) and BCD (B). C) The 1:2 m-THPC/BCD complex in which m-THPC is represented with ball and sticks while BCD as transparent surfaces. D) Illustration of the whole simulation box including the lipid bilayer, water bulk, the m-THPC/BCD complex and K^+, Cl^- ions.

Recently, by using both molecular modeling and simulations and experimental approaches,[36–38] we have shown that m-THPC is able to persistently interact with lipid bilayers, mimicking cellular or mitochondrial membranes. This leads to favorable conditions for PDT, since the drug can activate $^1O_2$ close to the potentially reactive target, i.e. the oxidizable lipid double bond. We have also shown that m-THPC can be easily and persistently encapsulated in a 1:2 ratio by β-cyclodextrin derivatives.[36,37] The latter represents a strategy which could limit aggregation and, thus, strongly enhance bioavailability. By using spectroscopic titration, the thermodynamic favorable encapsulation process has also been characterized in terms of its binding free energy.[37] Furthermore, we have shown that encapsulation takes place by an asynchronous mechanism

involving the sequential inclusion of the two cyclodextrin units.[37] On the other hands, we have confirmed that encapsulation is not altering the optical and photophysical properties of m-THPC, thus maintaining its ideal properties for PDT applications.[36] This observation is also confirmed by the fact that cyclodextrin-encapsulated m-THPC is highly cytotoxic or toxic under irradiation.[39–41]

Yet, the precise mechanisms through which encapsulated m-THPC is interacting with biological systems, such as lipid bilayers, has not been characterized yet. This concerns in particular the drug internalization and its release in the proximity of the cellular membrane, as well the accessibility of molecular oxygen, which is a crucial parameter to allow $^1O_2$ activation and efficient PDT applications. To this aim, we have performed long-scale all atom molecular dynamic (MD) simulations exceeding the μs time-scale of a β-cyclodextrin (BCD) encapsulated m-THPC interacting with a phosphatidylcholine (POPC) lipid bilayer surrounded by a water buffer and physiological salt concentration (Figure 1). The lipids have been modeled using the amberff21 force field,[42] while cyclodextrin and m-THPC force fields are the same as those used in our previous contributions.[36] All the simulations have been performed using the NAMD code[43,44] and visualized and analyzed with VMD,[45] initial systems have been built using the Charmm-Gui web interface,[46] and two independent replicates have been performed. Extended computational details can be found in Electronic Supplementary Information (ESI). Coherently with our previous work, the 1:2 m-THPC/BCD complex is highly stable in the water bulk (see ESI), confirming a suitable internalization.

Instead, as can be seen from the snapshots collected in Figure 2, the m-THPC/BCD complex, which was initially placed in the water bulk, is rapidly interacting with the lipid bilayer. After about 15 ns, the complex reaches the polar head region and develops interactions at the water/lipid

interface. This can also be appreciated by the distortion of the membrane surface, which forms a convex area in the vicinity of the m-THPC/BCD complex. However, this situation is evolving quite rapidly, and after about 30 ns the complex is buried deeper in the polar head region. Interestingly, in this state the deformation of the lipid membrane remains quite pronounced. Rather surprisingly, in the 180-250 ns range we observe that the m-THPC/BCD complex is actually spontaneously penetrating inside the lipid bilayer without experiencing any dissociation of its constitutive units. This spontaneous penetration is also confirmed by the second replicate, adding to the statistical significance of our interpretation (see ESI). This behavior was unexpected, especially considering the relatively large size of the complex and the rather hydrophilic propensities of cyclodextrin. Yet, the passive internalization of the drug-delivering unit should be regarded as highly beneficial for PDT, and in general for pharmacological applications.

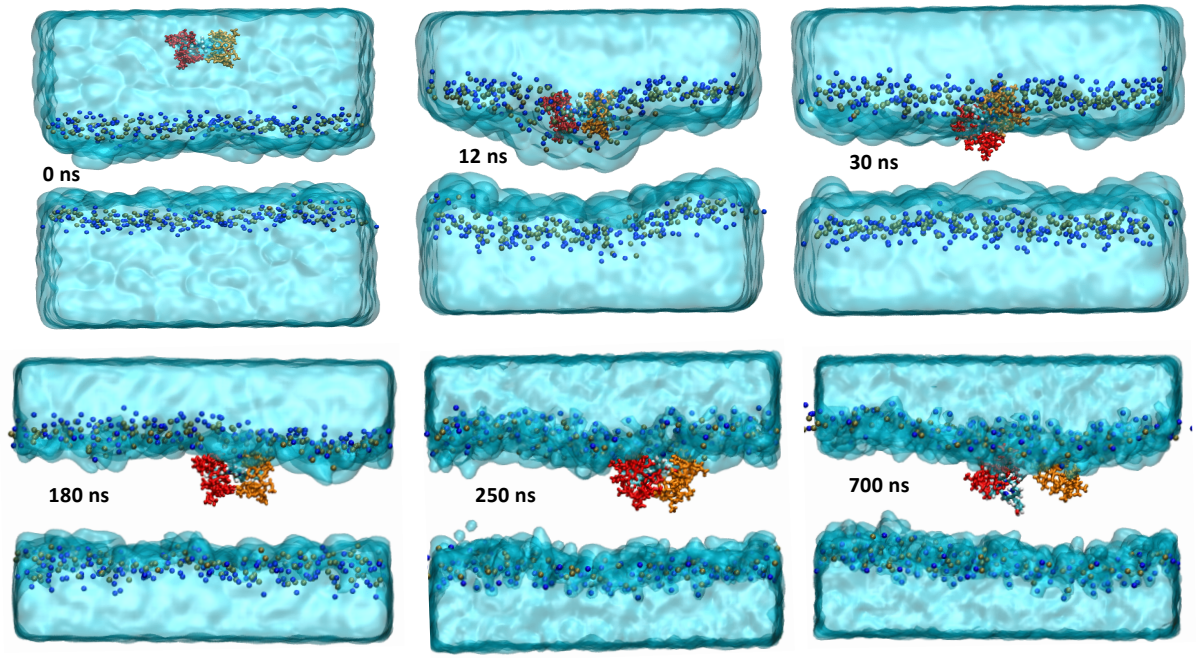

Figure 2. Snapshots extracted along the MD simulation showing the internalization of the m-THPC/BCD complex and its spontaneous dissociation in the lipid bilayer.

Once the internalization is completed, the complex still resides in the vicinity of the polar head region, experiencing some important rotational flexibility, most probably to maximize the interactions between the polar groups and the cyclodextrin components. However, after some hundreds of ns from the internalization (at about 450 ns) we can observe a major reorganization. Indeed, the strong interactions of the BCD units with the polar heads actually induces the opening of the complex, its partial dissociation and, thus, the exposure of the m-THPC core to the hydrophobic lipid environment. This behavior can also be appreciated by analyzing the time evolution of the distance between the center of mass of m-THPC and the two BCD units (Figure 3A) which shows a first partial release of one BCD. Indeed, the distance of BCD from m-THPC firstly increases to around 10 Å from 200 to 500 ns, indicating the partial opening of the complex, which is then followed by a sharp discontinuity indicative of the complete release of the BCD, with the distance reaching more than 18-20 Å.

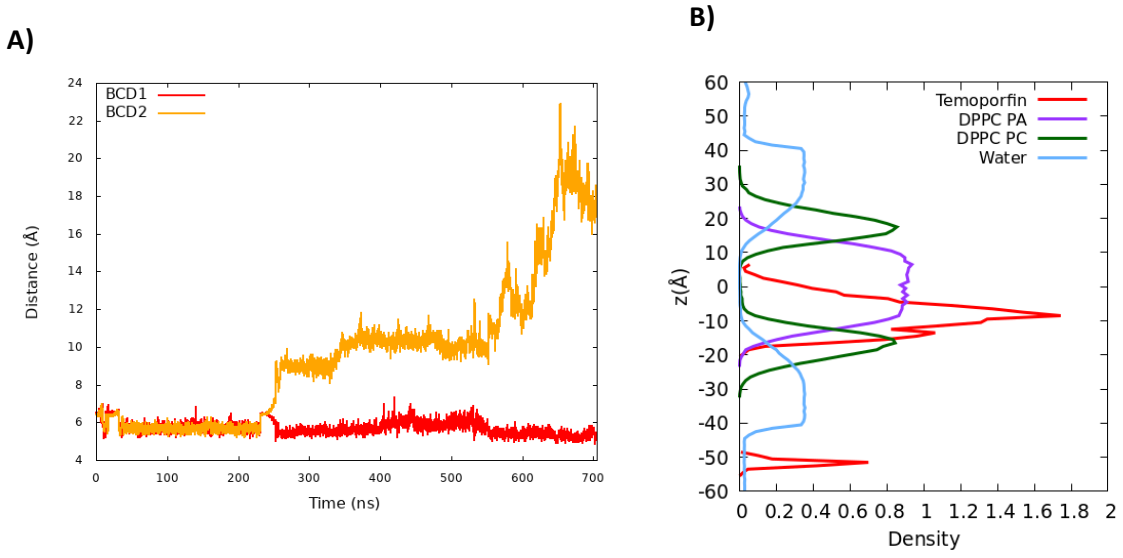

Figure 3. A) Time series of the distance between the centers of mass of m-THPC and the two BCD units. B) Density profile along the membrane axis of m-THPC, BCD, and lipid polar heads. The

secondary peak of m-THPC is representative of the pre-equilibrated situation in which the complex is in the water bulk.

The time scale of our MD simulation is not sufficient to enforce the spontaneous release of the second BCD unit, yet we may hypothesize that this process should take place given the affinity of the partially exposed m-THPC for hydrophobic environments. On the other hand, even the partial opening of the m-THPC/BCD complex is actually sufficient to allow the encounter between the chromophore and membrane-dissolved molecular oxygen, which is necessary for energy transfer and hence $^1O_2$ activation. Interestingly, as shown from the density profile along the membrane axis (Figure 3B), m-THPC is located close to the lipid reactive double-bonds, partially overlapping with their distribution, hence assuring the production of singlet oxygen in close proximity to its chemical target, and, consequently, decreasing the possibility of quenching.

In Figure 4 we also report the time evolution of some membrane structural parameters, obtained using the MEMBPLUGIN extension of VMD,[47] namely the area per lipid and the membrane thickness. Interestingly, and despite the local strong perturbation, we may observe only limited deviation from ideality for the two descriptors. The membrane thickness is slightly decreasing compared to the initial situation representative of an equilibrated bilayer and rapidly stabilizes at around 38 Å. On the other hand, the area per lipid is initially decreasing, corresponding to the formation of the pre internalized complex which is accompanied by a strong local deformation of the membrane. After the internalization, as can be expected the area per lipid slightly increases by 3-4 $Å^2$ with respect to an equilibrated membrane, and despite some oscillations it remains globally stable all along the MD simulation.

These data confirm that the internalization of the m-THPC complex is not accompanied by a strong perturbation of the bilayer. This aspect should also contribute to keep the drug toxicity in the dark at a relatively modest level, further confirming its suitability for PDT applications.

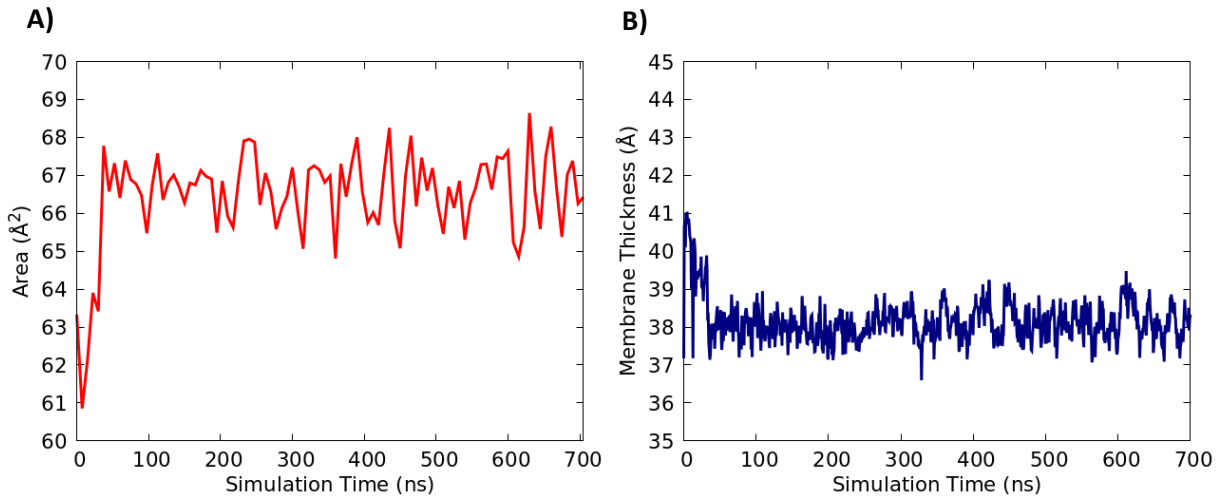

Figure 4. Time evolution of the area per lipid (Å) and membrane thickness (B) along the MD simulation.

The main interactions leading to both the complex internalization and dissociation involve the polar head and the peripheral substituents of the BCD complex as highlighted in Figure 5. Indeed, we may highlight that the dissociation proceeds through a subtle balance of hydrophobic and hydrophilic interactions involving the BCD complex and the nearby lipids. Specifically, after an initial step in which the lipid polar head, and particularly the $N(CH_3)^+$ moiety, of one lipid chain interacts with the methoxy oxygens of the cyclodextrin, thus driving the recognition (Figure 5A, D), a short lived state is formed. In the latter state the involved hydrophobic lipid tail interacts strongly with the BCD core and particularly inserts in the interface region between the two cyclodextrin units (Figure 5B, E). Afterwards, and following the partial dissociation of the

complex, m-THPC is stabilized by diverse factors involving cation-π interactions between the lipid polar heads and the peripheral phenyl rings, and π-alkyl interactions exerted by the hydrophobic tail (Figure 5C, F). Clearly the presence of the lipid tails and globally the lipid amphiphilic character disrupt the interaction network stabilizing the BCD/m-THPC complex, more importantly the stabilization of the exposed m-THPC and its novel interaction network hamper the subsequent reformation of the complex, making its opening irreversible. As concerns the second BCD unit its methoxy oxygen atoms also form favorable interactions with the polar head, contributing to keep this unit firmly anchored to the interface region.

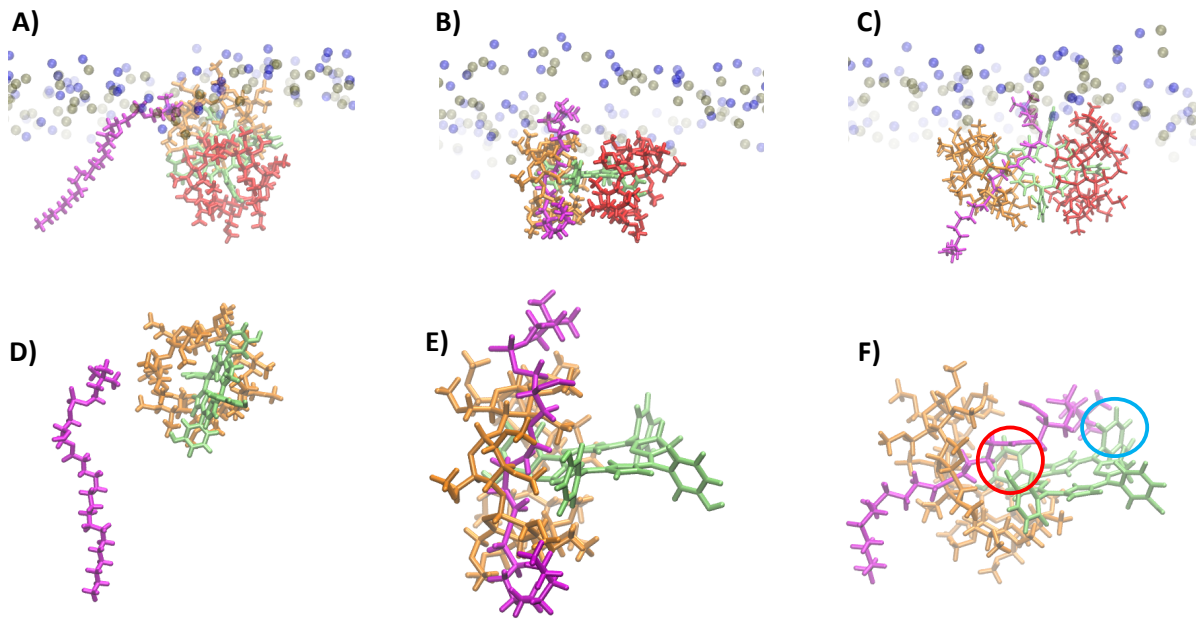

Figure 5. Main interactions developed by the m-THPC/BCD complex and the lipid polar heads leading to the complex partial dissociation. A) interaction between BCD and the polar head of one lipid chain leading to recognition, B) insertion of the lipid tail in the interface region between the BCD units destabilizing the complex, C) stabilization of the exposed m-THPC by interactions with the lipid tail and polar head. Zooms of the previous states are also provided in panel D

(recognition), E (complex destabilization), and F (m-THPC stabilization). Note that in panels D-F only the opening BCD is represented. The formation of cation-π and π-alkyl interactions are highlighted in panel F by red and blue circles, respectively.

By using long-scale all atom MD simulation we have shed light on the drug delivering propensity of a cyclodextrin-complexed temoporfin agent, which is clinically used in PDT application. In particular, and rather surprisingly, we have shown that the drug-delivering complex not only interacts with the lipid polar head but also leads to the spontaneous internalization of the complex in the hundreds of ns time-scale. Even more surprisingly, we have shown that the internalized complex, is no more stable and the locking of one cyclodextrin at the polar head combined with the hydrophobic affinity of temoporfin for the lipid core leads to its spontaneous partial dissociation. The whole process happens in a sub-μs time-scale and, thus, should be extremely biologically relevant. Furthermore, the combined effect of spontaneous internalization and dissociation is extremely beneficial and can justify the efficiency of the cyclodextrin-based vectorization in PDT. Indeed, while cyclodextrin is encapsulating and protecting the chromophore in water environment, notably avoiding unsuitable aggregation, it also readily frees temoporfin in the presence of its target, i.e. lipid membranes, making it accessible to molecular oxygen which can be activated to $^1O_2$ by subsequent energy transfer.

While our study represents a first explanation at molecular and atomistic level of the subtle interplay leading to drug-delivering and vectorization in PDT applications, it also allows to better understand the molecular factors driving the interaction with lipid bilayer, which can be further optimized in a rational molecular design approach. In particular, the possibility to decorate the cyclodextrin with specific moieties, such as antibodies or peptides, specifically overexpressed in

cancer cells is particularly attractive to enhance the selective deliver of the PDT agents, and will make the object of a further contribution.

ASSOCIATED CONTENT

Extended computational methodology, RMSD of the lipid and ligands, time series of the most important distances describing the interaction leading to the BCD opening. (file type, PDF)

AUTHOR INFORMATION

The authors declare no competing financial interests.

ACKNOWLEDGMENT

The authors thank GENCI and Explor as well as TUBITAK ULAKBIM High Performance and Grid Computing Center (TRUBA resources) and National Center for High Performance Computing of Turkey (UHeM) under grant number 1011062021 for computational resources. BKF and SC thank TUBITAK (Project Number: 120Z659) for financial support. BKF would also like to thank the French Embassy in Turkey for a joint Ph.D. grant. A.M. thanks ANR and CGI for their financial support of this work through Labex SEAM ANR 11 LABX 086, ANR 11 IDEX 05 02. The support of the IdEx "Université Paris 2019" ANR-18-IDEX-0001 and of the Platform P3MB is gratefully acknowledged.

REFERENCES

(1) Allison, R. R.; Downie, G. H.; Cuenca, R.; Hu, X. H.; Childs, C. J. H.; Sibata, C. H. Photosensitizers in Clinical PDT. *Photodiagnosis Photodyn. Ther.* **2004**, *1* (1), 27–42. https://doi.org/10.1016/S1572-1000(04)00007-9.

(2) Yanovsky, R. L.; Bartenstein, D. W.; Rogers, G. S.; Isakoff, S. J.; Chen, S. T. Photodynamic Therapy for Solid Tumors: A Review of the Literature. *Photodermatol. Photoimmunol. Photomed.* **2019**, *35* (5), 295–303. https://doi.org/10.1111/phpp.12489.

(3) Huang, Z.; Xu, H.; Meyers, A. D.; Musani, A. I.; Wang, L.; Tagg, R.; Barqawi, A. B.; Chen, Y. K. Photodynamic Therapy for Treatment of Solid Tumors--Potential and Technical Challenges. *Technol. Cancer Res. Treat.* **2008**, *7* (4), 309–320. https://doi.org/10.1016/j.bbi.2008.05.010.

(4) Yano, S.; Hirohara, S.; Obata, M.; Hagiya, Y.; Ogura, S.; Ikeda, A.; Kataoka, H.; Tanaka, M.; Joh, T. Current States and Future Views in Photodynamic Therapy. *J. Photochem. Photobiol. C Photochem. Rev.* **2011**, *12* (1), 46–67. https://doi.org/https://doi.org/10.1016/j.jphotochemrev.2011.06.001.

(5) Abrahamse, H.; Hamblin, M. R. New Photosensitizers for Photodynamic Therapy. *Biochemical Journal*. 2016, pp 347–364. https://doi.org/10.1042/BJ20150942.

(6) Ormond, A. B.; Freeman, H. S. Dye Sensitizers for Photodynamic Therapy. *Materials (Basel)*. **2013**, *6* (3), 817–840. https://doi.org/10.3390/ma6030817.

(7) Dasari, S.; Tchounwou, P. B. Cisplatin in Cancer Therapy : Molecular Mechanisms of Action. *Eur J Pharmacol* **2015**, *5* (0), 364–378.

(8) Forgie, B. N.; Prakash, R.; Telleria, C. M. Revisiting the Anti-Cancer Toxicity of Clinically Approved Platinating Derivatives. *Int. J. Mol. Sci.* **2022**, *23* (23). https://doi.org/10.3390/ijms232315410.

(9) Brown, J. M. Tumor Microenvironment and the Response to Anticancer Therapy. *Cancer Biology and Therapy*. Taylor & Francis September 2002, pp 453–458. https://doi.org/10.4161/cbt.1.5.157.

(10) Zahreddine, H.; Borden, K. L. B. Mechanisms and Insights into Drug Resistance in Cancer. *Frontiers in Pharmacology*. 2013, p 28. https://doi.org/10.3389/fphar.2013.00028.

(11) Dougherty, T. J.; Marcus, S. L. Photodynamic Therapy. *Eur. J. Cancer* **1992**, *28* (10), 1734–1742. https://doi.org/10.1016/0959-8049(92)90080-L.

(12) Bu, Y.; Xu, T.; Zhu, X.; Zhang, J.; Wang, L.; Yu, Z.; Yu, J.; Wang, A.; Tian, Y.; Zhou, H.; Xie, Y. A NIR-I Light-Responsive Superoxide Radical Generator with Cancer Cell Membrane Targeting Ability for Enhanced Imaging-Guided Photodynamic Therapy. *Chem. Sci.* **2020**, *11* (37), 10279–10286. https://doi.org/10.1039/d0sc03093g.

(13) Nyman, E. S.; Hynninen, P. H. Research Advances in the Use of Tetrapyrrolic Photosensitizers for Photodynamic Therapy. *J. Photochem. Photobiol. B Biol.* **2004**, *73* (1–2), 1–28. https://doi.org/10.1016/j.jphotobiol.2003.10.002.

(14) Kou, J.; Dou, D.; Yang, L. Porphyrin Photosensitizers in Photodynamic Therapy and Its Applications. *Oncotarget* **2017**, *8* (46), 81591–81603. https://doi.org/10.18632/oncotarget.20189.

(15) Koca, B.; Hamuryudan, E.; Catak, S.; Erdogmus, A.; Monari, A.; Aviyente, V. Exploring the Photophysics of Polyfluorinated Phthalocyanine Derivatives as Potential Theranostic Agents. *J. Phys. Chem. C* **2019**, *123* (40), 24417–24425. https://doi.org/10.1021/acs.jpcc.9b07053.

(16) Karges, J. Clinical Development of Metal Complexes as Photosensitizers for Photodynamic Therapy of Cancer. *Angew. Chemie - Int. Ed.* **2022**, *61* (5). https://doi.org/10.1002/anie.202112236.

(17) Dai, T.; Huang, Y. Y.; Hamblin, M. R. Photodynamic Therapy for Localized Infections-State of the Art. *Photodiagnosis and Photodynamic Therapy*. 2009, pp 170–188. https://doi.org/10.1016/j.pdpdt.2009.10.008.

(18) Koshi, E.; Mohan, A.; Rajesh, S.; Philip, K. Antimicrobial Photodynamic Therapy: An Overview. *J. Indian Soc. Periodontol.* **2011**, *15* (4), 323. https://doi.org/10.4103/0972-124X.92563.

(19) Gallardo-Villagrán, M.; Leger, D. Y.; Liagre, B.; Therrien, B. Photosensitizers Used in the Photodynamic Therapy of Rheumatoid Arthritis. *Int. J. Mol. Sci.* **2019**, *20* (13). https://doi.org/10.3390/ijms20133339.

(20) Makuch, S.; Dróżdż, M.; Makarec, A.; Ziółkowski, P.; Woźniak, M. An Update on Photodynamic Therapy of Psoriasis—Current Strategies and Nanotechnology as a Future Perspective. *Int. J. Mol. Sci.* **2022**, *23* (17). https://doi.org/10.3390/ijms23179845.

(21) Fan, W.; Huang, P.; Chen, X. Overcoming the Achilles' Heel of Photodynamic Therapy. *Chemical Society Reviews*. Royal Society of Chemistry December 7, 2016, pp 6488–6519. https://doi.org/10.1039/c6cs00616g.

(22) Wang, X.; Luo, D.; Basilion, J. P. Photodynamic Therapy: Targeting Cancer Biomarkers for the Treatment of Cancers. *Cancers (Basel).* **2021**, *13* (12). https://doi.org/10.3390/cancers13122992.

(23) Hayashi, N.; Kataoka, H.; Yano, S.; Tanaka, M.; Moriwaki, K.; Akashi, H.; Suzuki, S.; Mori, Y.; Kubota, E.; Tanida, S.; Takahashi, S.; Joh, T. A Novel Photodynamic Therapy Targeting Cancer Cells and Tumor-Associated Macrophages. *Mol. Cancer Ther.* **2015**, *14* (2), 452–460. https://doi.org/10.1158/1535-7163.MCT-14-0348.

(24) Hong, E. J.; Choi, D. G.; Shim, M. S. Targeted and Effective Photodynamic Therapy for Cancer Using Functionalized Nanomaterials. *Acta Pharm. Sin. B* **2016**, *6* (4), 297–307. https://doi.org/10.1016/j.apsb.2016.01.007.

(25) Senge, M. O.; Brandt, J. C. Temoporfin (Foscan®, 5,10,15,20-Tetra(m-Hydroxyphenyl)Chlorin) - A Second-Generation Photosensitizer. *Photochem. Photobiol.* **2011**, *87* (6), 1240–1296. https://doi.org/10.1111/j.1751-1097.2011.00986.x.

(26) Lange, C.; Lehmann, C.; Mahler, M.; Bednarski, P. J. *Comparison of Cellular Death Pathways after MTHPC-Mediated Photodynamic Therapy (PDT) in Five Human Cancer Cell Lines*; 2019; Vol. 11. https://doi.org/10.3390/cancers11050702.

(27) Wiehe, A.; Senge, M. O. The Photosensitizer Temoporfin (MTHPC) – Chemical, Pre-Clinical and Clinical Developments in the Last Decade†‡. *Photochem. Photobiol.* **2023**, *99* (2), 356–419. https://doi.org/10.1111/php.13730.

(28) Tan, I. B.; Dolivet, G.; Ceruse, P.; Poorten, V. Vander; Roest, G.; Rauschning, W. Temoporfin-Mediated Photodynamic Therapy in Patients with Advanced, Incurable Head and Neck Cancer: A Multicenter Study. *Head Neck* **2010**, *32* (12), 1597–1604. https://doi.org/10.1002/hed.21368.

(29) Düzgüneş, N.; Piskorz, J.; Skupin-Mrugalska, P.; Yıldırım, M.; Sessevmez, M.; Cheung, J.

Photodynamic Therapy of Oral Cancer and Novel Liposomal Photosensitizers. *Oral* **2023**, *3* (3), 276–294. https://doi.org/10.3390/oral3030023.

(30) Golusiński, P.; Szybiak, B.; Wegner, A.; Pazdrowski, J.; Pieńkowski, P. Photodynamic Therapy in Palliative Treatment of Head and Neck Cancer. *Otolaryngol. Pol.* **2015**, *69* (3), 12–17. https://doi.org/10.5604/00306657.1156330.

(31) Kurnit, K. C.; Fleming, G. F.; Lengyel, E. Updates and New Options in Advanced Epithelial Ovarian Cancer Treatment. *Obstet. Gynecol.* **2021**, *137* (1), 108–121. https://doi.org/10.1097/AOG.0000000000004173.

(32) Petri, A.; Yova, D.; Alexandratou, E.; Kyriazi, M.; Rallis, M. Comparative Characterization of the Cellular Uptake and Photodynamic Efficiency of Foscan® and Fospeg in a Human Prostate Cancer Cell Line. *Photodiagnosis Photodyn. Ther.* **2012**, *9* (4), 344–354. https://doi.org/10.1016/j.pdpdt.2012.03.008.

(33) Rezzoug, H.; Bezdetnaya, L.; A'amar, O.; Merlin, J. L.; Guillemin, F. Parameters Affecting Photodynamic Activity of Foscan® or Meta-Tetra(Hydroxyphenyl)Chlorin (MTHPC) in Vitro and in Vivo. *Lasers Med. Sci.* **1998**, *13* (2), 119–125. https://doi.org/10.1007/s101030050064.

(34) Millard, M.; Yakavetsa, I.; Piffoux, M.; Brun, A.; Gazeau, F.; Guigner, J. M.; Jasniewski, J.; Lassalle, H. P.; Wilhelm, C.; Bezdetnaya, L. MTHPC-Loaded Extracellular Vesicles Outperform Liposomal and Free MTHPC Formulations by an Increased Stability Drug Delivery Efficiency and Cytotoxic Effect in Tridimensional Model of Tumors. *Drug Deliv.* **2018**, *25* (1), 1790–1801. https://doi.org/10.1080/10717544.2018.1513609.

(35) Yakavets, I.; Millard, M.; Zorin, V.; Lassalle, H. P.; Bezdetnaya, L. Current State of the Nanoscale Delivery Systems for Temoporfin-Based Photodynamic Therapy: Advanced Delivery Strategies. *J. Control. Release* **2019**, *304* (May), 268–287. https://doi.org/10.1016/j.jconrel.2019.05.035.

(36) Aslanoglu, B.; Yakavets, I.; Zorin, V.; Lassalle, H. P.; Ingrosso, F.; Monari, A.; Catak, S. Optical Properties of Photodynamic Therapy Drugs in Different Environments: The Paradigmatic Case of Temoporfin. *Phys. Chem. Chem. Phys.* **2020**, *22* (29), 16956–16964. https://doi.org/10.1039/d0cp02055a.

(37) Yakavets, I.; Lassalle, H. P.; Yankovsky, I.; Ingrosso, F.; Monari, A.; Bezdetnaya, L.; Zorin, V. Evaluation of Temoporfin Affinity to β-Cyclodextrins Assuming Self-Aggregation. *J. Photochem. Photobiol. A Chem.* **2018**, *367* (August), 13–21. https://doi.org/10.1016/j.jphotochem.2018.07.046.

(38) Yakavets, I.; Yankovsky, I.; Bezdetnaya, L.; Zorin, V. Soret Band Shape Indicates MTHPC Distribution between β-Cyclodextrins and Serum Proteins. *Dye. Pigment.* **2017**, *137*, 299–306. https://doi.org/10.1016/j.dyepig.2016.11.007.

(39) Yakavets, I.; Millard, M.; Lamy, L.; Francois, A.; Scheglmann, D.; Wiehe, A.; Lassalle, H. P.; Zorin, V.; Bezdetnaya, L. Matryoshka-Type Liposomes Offer the Improved Delivery of Temoporfin to Tumor Spheroids. *Cancers (Basel).* **2019**, *11* (9), 1–16. https://doi.org/10.3390/cancers11091366.

(40) Yankovsky, I.; Bastien, E.; Yakavets, I.; Khludeyev, I.; Lassalle, H. P.; Gräfe, S.; Bezdetnaya, L.; Zorin, V. Inclusion Complexation with β-Cyclodextrin Derivatives Alters

Photodynamic Activity and Biodistribution of Meta-Tetra(Hydroxyphenyl)Chlorin. *Eur. J. Pharm. Sci.* **2016**, *91*, 172–182. https://doi.org/10.1016/j.ejps.2016.06.012.

(41) Yakavets, I.; Yankovsky, I.; Millard, M.; Lamy, L.; Lassalle, H. P.; Wiehe, A.; Zorin, V.; Bezdetnaya, L. The Alteration of Temoporfin Distribution in Multicellular Tumor Spheroids by β-Cyclodextrins. *Int. J. Pharm.* **2017**, *529* (1–2), 568–575. https://doi.org/10.1016/j.ijpharm.2017.07.037.

(42) Dickson, C. J.; Madej, B. D.; Skjevik, Å. A.; Betz, R. M.; Teigen, K.; Gould, I. R.; Walker, R. C. Lipid14: The Amber Lipid Force Field. *J. Chem. Theory Comput.* **2014**, *10* (2), 865–879. https://doi.org/10.1021/ct4010307.

(43) Phillips, J. C.; Braun, R.; Wang, W.; Gumbart, J.; Tajkhorshid, E.; Villa, E.; Chipot, C.; Skeel, R. D.; Kalé, L.; Schulten, K. Scalable Molecular Dynamics with NAMD. *J. Comput. Chem.* **2005**, *26* (16), 1781–1802. https://doi.org/10.1002/jcc.20289.

(44) Phillips, J. C.; Hardy, D. J.; Maia, J. D. C.; Stone, J. E.; Ribeiro, J. V.; Bernardi, R. C.; Buch, R.; Fiorin, G.; Hénin, J.; Jiang, W.; McGreevy, R.; Melo, M. C. R.; Radak, B. K.; Skeel, R. D.; Singharoy, A.; Wang, Y.; Roux, B.; Aksimentiev, A.; Luthey-Schulten, Z.; Kalé, L. V.; Schulten, K.; Chipot, C.; Tajkhorshid, E. Scalable Molecular Dynamics on CPU and GPU Architectures with NAMD. *J. Chem. Phys.* **2020**, *153* (4), 044130. https://doi.org/10.1063/5.0014475.

(45) Humphrey, W.; Dalke, A.; Schulten, K. VMD: Visual Molecular Dynamics. *J. Mol. Graph.* **1996**, *14* (1), 33–38. https://doi.org/10.1016/0263-7855(96)00018-5.

(46) Jo, S.; Kim, T.; Iyer, V. G.; Im, W. CHARMM-GUI: A Web-Based Graphical User

Interface for CHARMM. *J. Comput. Chem.* **2008**, *29* (11), 1859–1865. https://doi.org/10.1002/jcc.20945.

(47) Guixà-González, R.; Rodriguez-Espigares, I.; Ramírez-Anguita, J. M.; Carrió-Gaspar, P.; Martinez-Seara, H.; Giorgino, T.; Selent, J. MEMBPLUGIN: Studying Membrane Complexity in VMD. *Bioinformatics* **2014**, *30* (10), 1478–1480. https://doi.org/10.1093/bioinformatics/btu037.